RESEARCH ARTICLE
doi: 10.2306/scienceasia1513-1874.2024.064

ScienceAsia 50 (3): 2024: ID 2024064: **1–7**

Evaluation of the antioxidant and anti-leukaemic effects of *Andrographis paniculata* methanol extract

Hoang Thanh Chi[a], **Vo Ngoc Tram**[b], **Nguyen Trung Quan**[b], **Bui Thi Kim Ly**[a,*]

[a] Department of Medicine and Pharmacy, Thu Dau Mot University, Thu Dau Mot, Binh Duong 820000 Vietnam
[b] Department of Biology and Biotechnology, VNU University of Science, Vietnam National University, Ho Chi Minh City 72711 Vietnam

*Corresponding author, e-mail: lybtk@tdmu.edu.vn

Received 25 Apr 2023, Accepted 1 May 2024
Available online 21 Jul 2024

ABSTRACT: *Andrographis paniculata* is widely used in traditional medicine for treating human diseases. Although there are many scientific reports on this plant's bio-effects, the lack of leukaemia inhibition impact still remains. In this study, *A. paniculata* methanol extract (MeAP) was investigated for its antioxidant capacity by DPPH and FRAP assays and for the anti-leukemic effect. The results showed that MeAP could scavenge the DPPH and donate an electron in the FRAP reaction. The cytotoxicity of MeAP was clarified as being strongly selective on Tel-TrkC fusion protein-associated Acute Myeloid Leukaemia (AML) cells with the $IC_{50} = 8.48 \pm 0.21$ µg/ml in a dependent manner of dose, time, and cell-density. Moreover, MeAP also inhibited Tel-TrkC phosphorylation.

KEYWORDS: *A. paniculata*, leukaemia, antioxidant, Tel-TrkC fusion protein

INTRODUCTION

Andrographis paniculata (Burm. f.) Wall. ex Nees (*A. paniculata*) is a herb widely used in folk remedies, especially in Southeast Asia [1]. Scientific evidence shows the diversity in phytochemical composition of the plant and the vigorous antioxidant activity of its extracts [2]. During the COVID-19 pandemic, the inhibitory impact of *A. paniculata* on the virus was determined; the related products have been materializing to ameliorate the disease sequelae [3, 4]. Other bio-activities of *A. paniculata* have also been recorded, including anti-cancer cell toxicity and treatment of malaria [5, 6]. As a medicinal plant with high diversity of bioactive constituents, it is proposed that the activities conferred by this herb extract may be the antioxidant activity through the electron tolerance of the andrographolide compound [7, 8]. The presence of secondary metabolites also contributes to the formation of cytotoxic activity. Despite popular studies, the effect of *A. paniculata* on leukaemia is still limited, especially in acute myeloid leukaemia (AML). The anticancer effects of this plant have been previously demonstrated, leading to predictions about its anti-leukaemia activity [6]. One of the important signaling pathways in leukaemia treatment is the signaling pathway of extracellular receptors [6]. Besides, a common fusion protein detected in leukaemia, Tel-TrkC, is also an agent closely related to AML [6, 9]. However, very few cases of AML associated with the Tel-TrkC fusion protein have been reported [9]. The rarity leads to limited studies on relevant topics, thereby, leading to a lack of scientific information for treating patients. The present study aimed to initially assess the antioxidant capacity and ability to inhibit cell proliferation on a model of AML harboring the *ETV6-NTRK3* fusion gene (encoding the Tel-TrkC fusion protein) of the methanol extract of *A. paniculata*.

MATERIALS AND METHODS

Herbal materials and extract preparation

A. paniculata shoot systems were harvested in August 2017 and identified by Dr. Dang Van My (voucher no. BNAG-2017-0115, Traditional Medicine Center, Tinh Bien District, An Giang Province, Vietnam). The harvested sample was washed, thoroughly dried at 40 °C, and ground into fine powder. A mass of dried powder was macerated into ten masses of absolute methanol. After four days of soaking, the filtrate was collected and deprived of the solvent by using a rotovap machine (EYELA 1L Rotary Evaporator, Shanghai, China) to obtain a crude extract. A stock of *A. paniculata* methanol extract (MeAP) (200 mg/ml) was prepared by weighting and dissolving the crude extract in dimethylsulfoxide (DMSO, Sigma-Aldrich, Missouri, USA). The MeAP stock was sterile-filtered, aliquoted, and stored at −20 °C until use.

Cell lines and cell culture conditions

An acute myeloid leukaemia cell line harboring the fusion Tel-TrkC, MO-91, was used to detect the anti-leukemic effect of MeAP [10], and a normal kidney cell, Vero, was a control model [11]. The MO-91 cell was cultured in Roswell Park Memorial Institute 1640 medium – RPMI (Sigma-Aldrich), while the Vero cell was cultured in Dulbecco's modified Eagle's medium – DMEM (Sigma-Aldrich) supplemented with 10% fetal bovine serum (Thermofisher Scientific, Massachusetts, USA), 100 IU/ml penicillin, and 0.1 mg/ml strepto-

mycin (Sigma-Aldrich) in a humidified incubator of 5% CO_2 at 37 °C.

α, α-diphenyl-β-picrylhydrazyl (DPPH) free radical scavenging assay

The DPPH assay was performed to determine the antioxidant capacity of MeAP [12]. A gradient of 0 to 1600 µg/ml MeAP was reacted with 0.3 mM DPPH (Sigma-Aldrich) at a proportion of 1:1 (v/v), incubated at 37 °C for 30 min, and absorbance measured at 517 nm using an ELISA reader (VersaMax ELISA Microplate Reader, Molecular Devices, California, USA). The antioxidant effect was exposed by the percentage of eliminated DPPH compared with input DPPH and calculated using the following equation: % DPPH radical scavenging = [(negative control—sample)/negative control]×100.

Ferric-ion-reducing antioxidant power (FRAP) assay

FRAP assay, a redox-linked colorimetric method [13] was used for the detection of total antioxidant power of the MeAP. A FRAP working reagent was prepared by mixing 300 mM acetate buffer pH 3.6 (3.1 g sodium acetate trihydrate (Sigma-Aldrich) was added into 16 ml glacial acetic acid, then made up to 1 l with distilled water), 10 ml TPTZ in 40 mM HCl, and 20 mM $FeCl_3 \cdot 6\,H_2O$ in a ratio of 10:1:1 at 37 °C. A volume of 5 µl MeAP was pipetted into 3995 µl working FRAP reagent and mixed thoroughly. After 4 min of incubation at room temperature, an absorbance of the MeAP at 593 nm was recorded by an ELISA reader (VersaMax ELISA Microplate Reader) against the blank. The reactions of solvent and Trolox (Sigma-Aldrich) were used as blank and calibration for this assay: FRAP value = (Abs sample/Abs calibration) × FRAP value of calibration.

Cytotoxicity effect of the MeAP

MO-91 biomass at a density of 10^5 cells/ml was seeded into a 6-well plate separately with and without MeAP at a concentration of 0 to 100 µg/ml and then incubated at 37 °C with 5% CO_2 for 48 h. The cell viability was measured by carrying out a Trypan blue exclusion test [14]. The cytotoxicity was observed, and the half-maximal inhibitory concentration (IC_{50}) was regressed.

Vero biomass was seeded into a 6-well plate at a density of 10^5 cells/ml. After 24 h of incubation at 37 °C with 5% CO_2, the MeAP was added to reach the final concentration range of 0 to 200 µg/ml. The MTT assay was conducted to calculate Vero cell viability [15]. The selective index (SI) was calculated as the quotient of the IC_{50} values of the MO-91 and the Vero cells, which depicted the selective impact on the cell of interest [16]. The MeAP (6.25 µg/ml) was further evaluated for its influence at different cell densities (10^4 to 10^6 cells/ml) and times of exposure (0 to 96 h).

TrkC expression under the influence of MeAP

MO-91 cells were cultured in DMEM supplemented with MeAP (0, 12.5, 25, or 50 µg/ml) at a density of 10^5 cells/ml. After 8 h of incubation at 37 °C with 5% CO_2, the cells were harvested and washed twice with DPBS (TBR Technology Co., Ho Chi Minh City, Vietnam). Total protein content was obtained by lysing the cells on ice using protein lysis buffer (10 mM disodium diphosphate, 50 mM fluoride, 5 mM ethylenediaminetetraacetic acid, 1 mM sodium orthovanadate, and 5 mM 4-(2-hydroxyethyl)-1-piperazineethanesulfonic acid, 1 mM phenylmethylsulfonyl fluoride, 0.01% Triton X-100, 150 mM sodium chloride, and 75 µg/ml aprotinin) [6]. 500 mg of the lysate was incubated with anti-TrkC (C-14) (1:500; cat. no. sc-11; Santa Cruz Biotechnology, California, USA) at 4 °C overnight, and then Protein G Sepharose 4 Fast Flow (Amersham Pharmacia Biosciences, Cytiva, Vancouver, Canada) was added to collect the immunoprecipitates following the user's manual. The sediment was triple-washed with Tris-buffered saline with Tween-20 before protein analytical expression by SDS-page electrography and western blotting with the anti-TrkC (C-14) and anti-phosphotyrosine 4G10 (1:1,000; cat. no. 05-321MG; Upstate Biotechnology, Merck, Massachusetts, USA) [17]. An anti-mouse IgG HRP (1:1,000; cat. no. sc-2031; Santa Cruz Biotechnology, California, USA), or an anti-rabbit IgG HRP (1:1,000; cat. no. sc-2317; Santa Cruz Biotechnology), was used as secondary antibodies.

Statistical analysis

Experiments were conducted independently at least three times. Data was illustrated as the mean ± SEM and statistically analyzed by using GraphPad Prism software ver. 8.3.0 with a significance level of 0.05.

RESULTS

The MeAP manifested the antioxidant capacity

A nonlinear regression was carried out to build a chart depicting the relationship between the MeAP concentration and the percentage of scavenged DPPH. The DPPH radicals were found to be trapped in the presence of MeAP. However, at the high concentration of MeAP (above 1000 µg/ml), the ratio of scavenged DPPH did not reach the 50% value, leading to the indeterminable EC_{50} (half maximal effective concentration) of MeAP on the DPPH assay (Fig. 1A).

The reducing power of MeAP was investigated as an auxiliary element to demonstrate the antioxidant action of the extract [18]. The FRAP value was translated from the relation between the test sample's absorbance and the known FRAP value's calibration [19]. The relative activity of Trolox was confirmed as

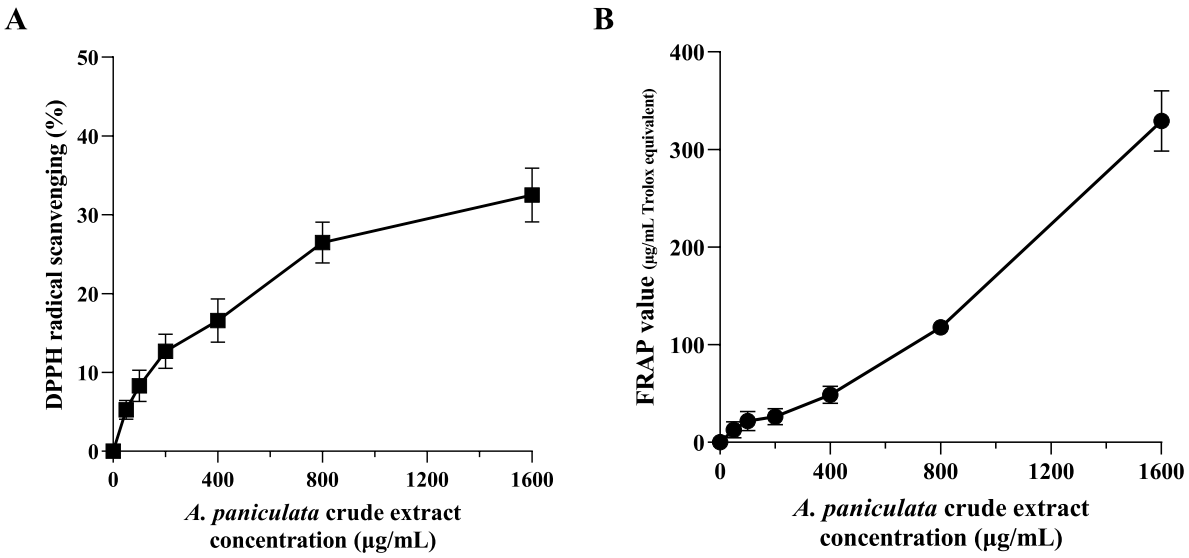

Fig. 1 Antioxidant capacity of MeAP recorded by (A) DPPH assay and (B) FRAP assay.

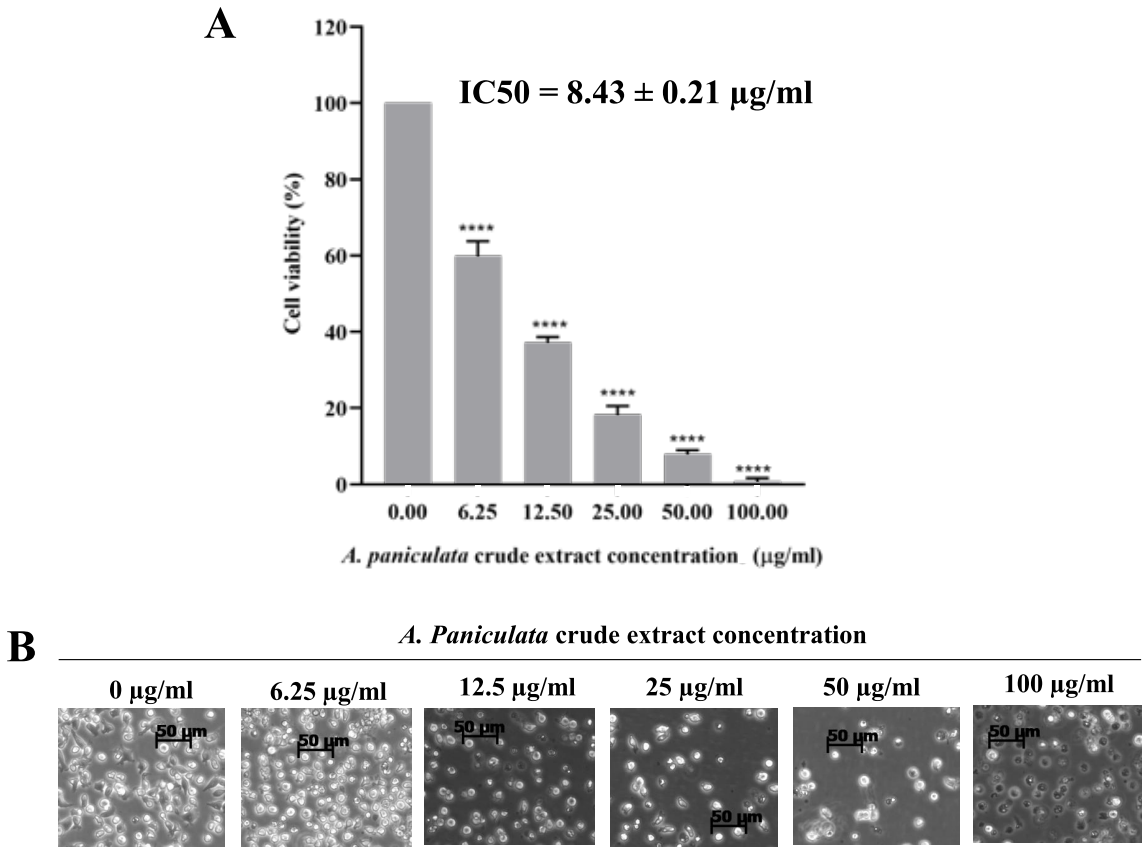

Fig. 2 Cytotoxicity of MeAP on MO-91 cells in dose-dependent manner (A) and cell morphology changed with the increasing extract concentration (B). (****): p-value < 0.0001.

2.0 to the direct reaction of Fe(II), which means that at the concentrations of 100 and 200 µM, the FRAP values of Trolox were 200 and 400 µM (Fig. 1B).

The anti-leukaemic effect of MeAP on MO-91 cells in a dose-dependent manner

The anti-leukaemic effect of MeAP was investigated on MO-91 cells. The cells were cultured in the presence of the extract at various final concentrations (6.25, 12.5, 25, 50, and 100 µg/ml). The cells that were untreated by the extract were negative controls. The ANOVA tests, followed by Tukey post hoc tests, were performed; and the result showed that there was a statistically significant difference between cell survival at different MeAP concentrations. The IC_{50} of the MeAP on MO-91 was clarified at 8.48 ± 0.21 µg/ml (Fig. 2A). Compared with the control group, the morphology of the MO-91 cells treated with MeAP was decreased in number and cell size, and cell debris appeared (Fig. 2B).

The anti-leukaemic effect of MeAP on MO-91 in a time-dependent manner

The experiments were conducted for up to 96 h of extract exposure. The MeAP at a concentration of 6.25 µg/ml was used for observation. The results showed that the cell population slightly increased in the first 48 h of incubation and, then, declined in the next 48 h. In contrast, cell proliferation in the negative control group was observed to grow normally (Fig. 3A). The morphology MeAP treated cells showed cell shrinkage, cell debris, and membrane blebbing (Fig. 3B).

The anti-leukaemic effect of MeAP on MO-91 in a cell density-dependent manner

MeAP at a concentration of 12.5 µg/ml was used for lethality validation of the extract on MO-91 cell density (10^4, 5×10^4, 10^5, 5×10^5, and 10^6 cells/ml). The cell density was clearly found to affect the cytotoxicity of the MeAP. The greater the initial cell density, the lower the lethal effect of the extract was recorded (Fig. 4A).

The cytotoxicity ability of MeAP was selective for the AML cell line

The MeAP in the concentration gradient (0 to 200 µg/ml) was investigated for toxicity on Vero cells. At the concentration of 100 µg/ml, the Vero cell viability stayed above the value of 50% (Fig. 5). The SI value was calculated by dividing the IC_{50} value of MeAP on MO-91 cells by the one on Vero cells, which clarified as 13.03.

The MeAP down-regulated the Tel-TrkC fusion protein activity

The TrkC immunoprecipitates were analyzed by TrkC antibody and 4G10 antibody conjugation. There was a sharp decrease in the protein band of phosphoryl TrkC, which hybridized with the 4G10 antibody in the co-culture of MeAP (Fig. 6A). On the other hand, the total TrkC content was unchanged during the test. For transformation clarification, the ImageJ (LOCI, University of Wisconsin) software was used to digitise protein bands' expressions [20]. The ratio of phosphoryl TrkC to total TrkC was detailed in Fig. 6B, showing a declining with the increasing MeAP concentration.

DISCUSSION

A. paniculata is commonly chosen for research projects because of its wide use in traditional medicine [1]. It was reported from a quantitative analysis that the main ingredients of this plant were carbohydrate (60.20%), protein (3.72%), crude fat (2.93%), moisture (3.00%), ash (2.71%), and crude fibre (27.46%) [7]. The GC-MS phytochemical screening results showed that this plant contains over 40 compounds divided into four groups, including the aromatic and terpenoid groups [8]. Previously, the high content of polyphenols was detected in *A. paniculata*, in which the phenolic content (mg of GAE/g) appeared the most in the fruit (181.00 ± 1.48), followed by the stem (55.02 ± 0.35) and the leaves (75.86 ± 0.82) [21]. The presence of polyphenols, especially flavonoids, is considered one of the main agents in antioxidant processes [22]. The EC_{50} of MeAP in the DPPH assay was above 1600 µg/ml which was inconsistent with the result of a previous study [23]. Because of their importance and diversity in phytochemical composition, phenolic compounds play an important role in the bioactivity of plant extracts, including their antioxidant capacity [24]. The association of related activities such as antioxidant and cytotoxicity has been noted in previous studies; the polyphenol content in the extract shows a relationship with cytotoxic activity [25, 26]. However, phenolic compounds were reported to vary depending on the season, growing time, and soil conditions, leading to differences in the activity of the plant extracts [27]. The antioxidant properties of the extract are also demonstrated through its ability to donate electrons, as reflected in reduction reactions [28]. In the present study, the reducing activity of MeAP was also recorded via the FRAP assay.

Under the activity of MeAP, the leukaemia cells vitality decreased. The cytotoxicity of the MeAP was in a dependent manner of dose, time, and cell-density. Thus far, the anticancer ability of *A. paniculata* has also been detected in several cancer types [5, 29–32]. The *A. paniculata*-derived dichloromethane factional extract had a lethal impact on colon cancer cells HT-29, but the extract enhanced the cell viability of the monocyte isolated from peripheral blood [5]. Moreover, andrographolide extracted from this plant directly inhibits p27 and CDK4, leading to the G0 cell arrest. Andrographolide also increases lymphocyte prolifer-

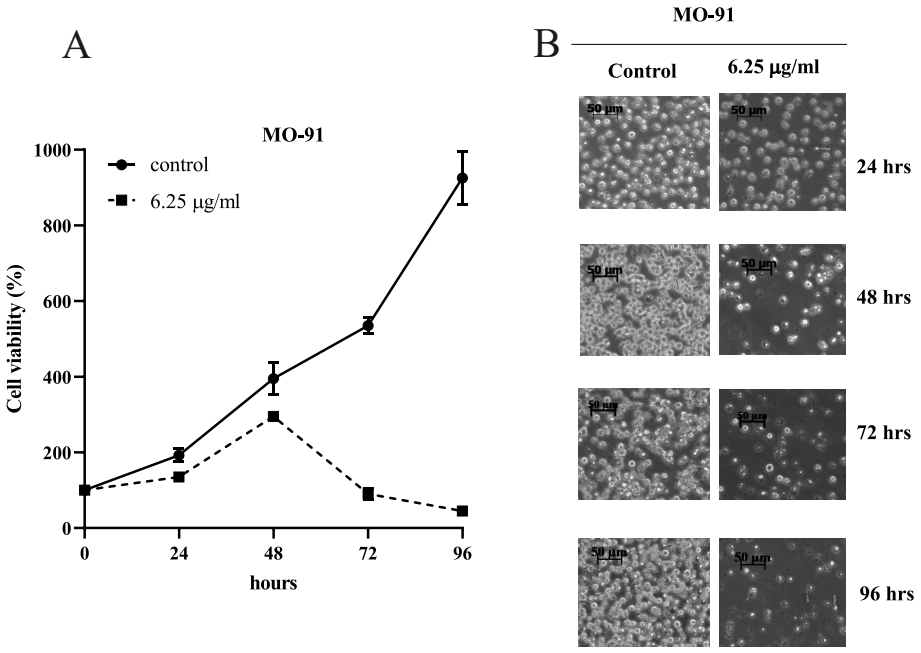

Fig. 3 Cytotoxicity of MeAP on MO-91 cells in time-dependent manner (A) and the cell morphology changed during the experiment (B).

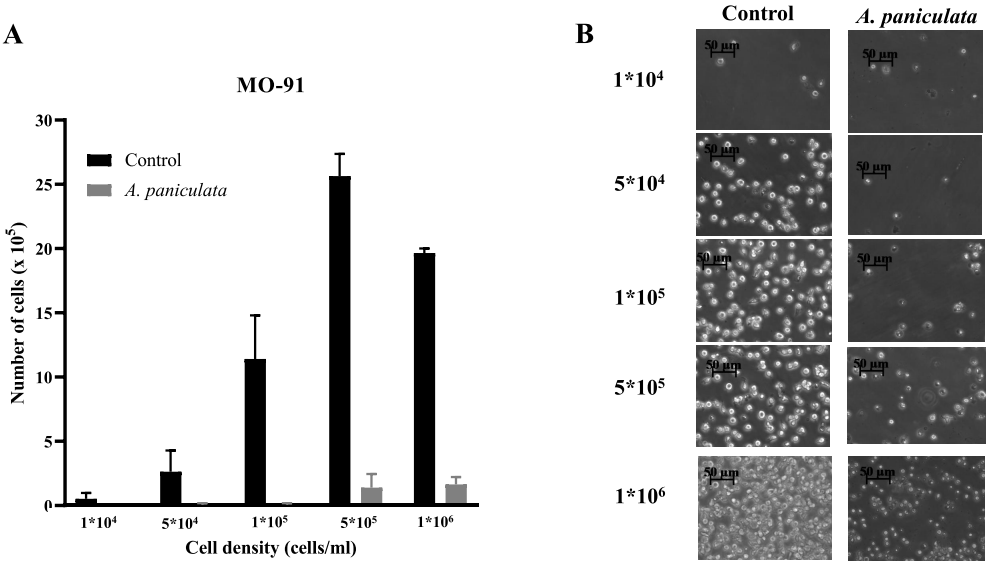

Fig. 4 Cytotoxicity of MeAP on MO-91 cells in cell density-dependent manner (A) and the cell density observed after the treatment (B).

ation. The pathways associated with NFκB, HER2, MMP9, and CXCR4 were recorded to be influenced by *A. paniculata* in Caco-2 cells [8]. The MeAP was classified as having a strong anti-leukemic effect due to its IC50 value being below 100 µg/ml in this study [33]. Moreover, the MeAP showed ineffective lethality on Vero cells, as illustrated by a IC_{50} value beyond 100 µg/ml [34]. Based on the IC_{50} values, the SI value of MeAP on AML cells was determined to be 13.03; the value was greater than 10, expressing the effect of MeAP as highly selective on tested leukaemia cells [16]. Previously, a diterpene lactone compound extracted from *A. paniculata* named andrographolide downregulated the Bcr-Abl and activated the level of Bax, causing apoptosis via an intrinsic inducing pathway [6]. The cell morphology changes during

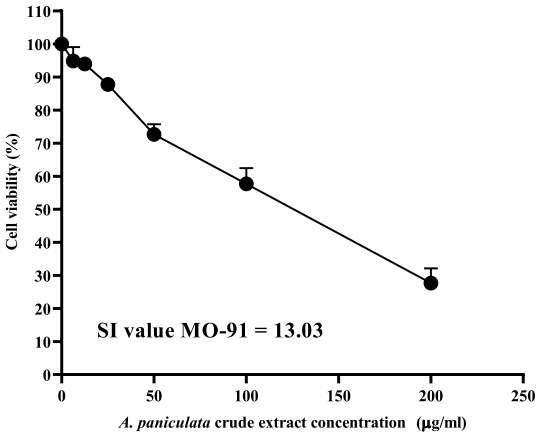

Fig. 5 Selective index in the effect of MeAP on MO-91 cell viability compared with the Vero cell's.

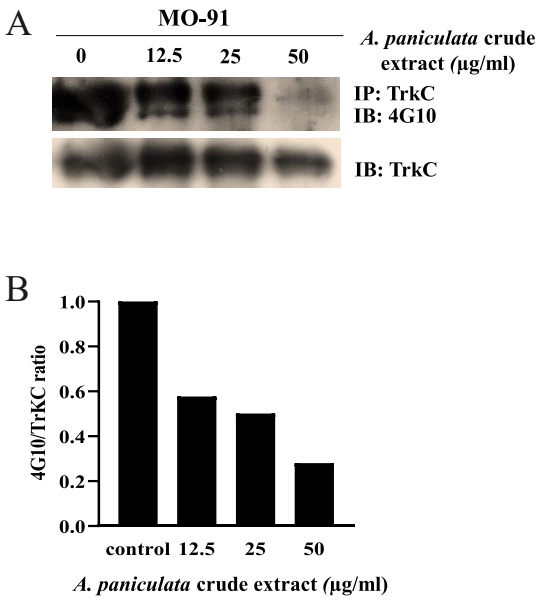

Fig. 6 TrkC phosphoryl down-regulation under the impact of MeAP in dose-dependent manner: (A) Protein hybridization result and (B) numericizing result.

the treatment revealed cell death pathways [35]. The permeability of the cell membrane and cell shrinkage, one of the most frequently predominant morphological properties of cell death apoptosis process observed in this study, needed further in-depth research to verify [35].

Cell cycle arrest, induction of apoptosis, anti-angiogenic behavior, and suppression of IL-6 expression are some of the impact strategies of *A. paniculata* extract [36]. Andrographolide was reported to inhibit the A549 cell model via sustained inactivation of PI3K and Akt signalling [37]. One of the upstreams of PI3K/Akt pathways in AML is the Tropomyosin receptor kinase (Trk) family encoded by *NTRK1*, *NTRK2*, and *NTRK3*. A fusion protein, Tel-TrkC, encoded by *NTRK3-ETV6*, causes AML because of self-phosphorylation [38]. In the acute myleoid leukaemia model U937, andrographolide induces apoptosis through the intracellular activation pathway [9]. Activation of intracellular apoptosis is reported to be triggered by receptor-mediated signals [35]. The association of leukaemic cell apoptosis with tyrosine receptors has been observed previously, typically with interactions on Bcr-Abl; The effect of cell apoptosis throuh Tel-TrkC could also be inferred [6]. Because the number of cases is quite small, scientific publications on *ETV6-NTRK3*-associated leukaemia are very limited [9]. MeAP-induced inhibition of TrkC phosphorylation was noticeable information. The phosphoryl-blocking activity of MeAP was dose-dependent. It suggested that the lethality effect of the extract was Tel-TrkC-mediated.

CONCLUSION

The *A. paniculata* methanol extract exhibited antioxidant activity, via the DPPH scavenging activity, and reduced the Fe^{3+} TPTZ complex. The cytotoxicity effect of the extract was discovered on AML cells by blocking the Tel-TrkC activity.

Acknowledgements: We are really appreciated Professor Yuko Sato (University of Tokyo, Japan) for providing the MO-91 cell line.

REFERENCES

1. Hossain MS, Urbi Z, Sule A, Hafizur Rahman KM (2014) *Andrographis paniculata* (Burm. f.) Wall. ex Nees: a review of ethnobotany, phytochemistry, and pharmacology. *Sci World J* **2014**, 274905–274905.
2. Mussard E, Cesaro A, Lespessailles E, Legrain B, Berteina-Raboin S, Toumi H (2019) Andrographolide, a natural antioxidant: An update. *Antioxidants (Basel)* **8**, 571.
3. Nguyen HT, Do VM, Phan TT, Nguyen Huynh DT (2023) The potential of ameliorating COVID-19 and sequelae from *Andrographis paniculata* via bioinformatics. *Bioinform Biol Insights* **17**, 11779322221149622.
4. Kaewdech A, Nawalerspanya S, Assawasuwannakit S, Chamroonkul N, Jandee S, Sripongpun P (2022) The use of *Andrographis paniculata* and its effects on liver biochemistry of patients with gastrointestinal problems in Thailand during the COVID-19 pandemic: a cross sectional study. *Sci Rep* **12**, 18213.
5. Ahmad M, Ahmad S, Arshad M, Afzal M (2014) *Andrographis paniculata* a miracle herbs for cancer treatment: *In vivo* and *in vitro* studies against Aflatoxin B1 toxicity. *Egypt J Med Hum Genet* **15**, 163–171.
6. Hodroj MH, Jardaly A, Abi Raad S, Zouein A, Rizk S (2018) Andrographolide potentiates the antitumor effect of topotecan in acute myeloid leukaemia cells through an intrinsic apoptotic pathway. *Cancer Manag Res* **10**, 1079–1088.
7. Adedapo AA, Adeoye BO, Sofidiya MO, Oyagbemi AA (2015) Antioxidant, antinociceptive and anti-inflammatory properties of the aqueous and ethanolic

leaf extracts of *Andrographis paniculata* in some laboratory animals. *J Basic Clin Physiol Pharmacol* **26**, 327–334.
8. Roy S, Rao K, Bhuvaneswari C, Narasu M, Giri A (2009) Phytochemical analysis of *Andrographis paniculata* extract and its antimicrobial activity. *World J Microbiol Biotechnol* **26**, 85–91.
9. Solomon JP, Benayed R, Hechtman JF, Ladanyi M (2019) Identifying patients with NTRK fusion cancer. *Ann Oncol* **30**, VIII16–VIII22.
10. Gu TL, Popova L, Reeves C, Nardone J, MacNeill J, Rush J, Nimer SD, Polakiewicz RD (2007) Phosphoproteomic analysis identifies the M0-91 cell line as a cellular model for the study of TEL-TRKC fusion-associated leukaemia. *Leukaemia* **21**, 563–566.
11. Ammerman NC, Beier-Sexton M, Azad AF (2008) Growth and maintenance of Vero cell lines. *Curr Protoc Microbiol* **11**, A4E1–A4E7.
12. Ly B, Nguyen Q, Dao L, Nguyen H, Lam M, Hoang C (2019) Evaluation of antimicrobial, antioxidant and cytotoxic activities of *Dialium cochinchinensis* seed extract. *Indian J Pharm Sci* **81**, 975–980.
13. Benzie IF, Strain JJ (1996) The ferric reducing ability of plasma (FRAP) as a measure of "antioxidant power": the FRAP assay. *Anal Biochem* **239**, 70–76.
14. Ly BT, Chi HT, Yamagishi M, Kano Y, Hara Y, Nakano K, Sato Y, Watanabe T (2013) Inhibition of FLT3 expression by green tea catechins in FLT3 mutated-AML cells. *PLoS One* **8**, e66378.
15. Ala AA, Olotu BB, Ohia CMD (2018) Assessment of cytotoxicity of leaf extracts of *Andrographis paniculata* and *Aspilia africana* on murine cells *in vitro*. *Arch Basic Appl Med* **6**, 61–65.
16. Mahavorasirikul W, Viyanant V, Chaijaroenkul W, Itharat A, Na-Bangchang K (2010) Cytotoxic activity of Thai medicinal plants against human cholangiocarcinoma, laryngeal and hepatocarcinoma cells *in vitro*. *BMC Complement Altern Med* **10**, 55.
17. Chi HT, Ly BTK (2022) Artemisia vulgaris inhibits BCR/ABL and promotes apoptosis in chronic myeloid leukaemia cells. *Biomed Rep* **17**, 92.
18. Cheng Z, Li Y (2004) Reducing power: the measure of antioxidant activities of reductant compounds? *Redox Rep* **9**, 213–217.
19. Benzie IF, Strain JJ (1999) Ferric reducing/antioxidant power assay: direct measure of total antioxidant activity of biological fluids and modified version for simultaneous measurement of total antioxidant power and ascorbic acid concentration. *Methods Enzymol* **299**, 15–27.
20. Collins TJ (2007) ImageJ for microscopy. *BioTechniques* **43**, S25–S30.
21. Rafat A, Philip K, Muniandy S (2010) Antioxidant potential and content of phenolic compounds in ethanolic extracts of selected parts of *Andrographis paniculata*. *J Med Plant Res* **4**, 197–202.
22. Kasote DM, Katyare SS, Hegde MV, Bae H (2015) Significance of antioxidant potential of plants and its relevance to therapeutic applications. *Int J Biol Sci* **11**, 982–991.
23. Nagalekshmi R, Menon A, Chandrasekharan DK, Nair CK (2011) Hepatoprotective activity of *Andrographis paniculata* and *Swertia chirayita*. *Food Chem Toxicol* **49**, 3367–3373.
24. Lin D, Xiao M, Zhao J, Li Z, Xing B, Li X, Kong M, Li L, et al (2016) An overview of plant phenolic compounds and their importance in human nutrition and management of type 2 diabetes. *Molecules* **21**, 1374.
25. Navakanitworakul R, Wanso D, Phetcharat S, Chumkaew P, Mayakun J (2023) Variations in total phenolics in *Sargassum plagiophyllum* and their cytotoxic activities. *ScienceAsia* **49**, 791–796.
26. Seubsasanaa S, Dechayontb B, Pipatrattanasereec W, Malisorn N (2023) Antioxidant activity, α-glucosidase inhibition, and phytochemical profiling of *Belosynapsis ciliata* (Blume) R.S.Rao extracts. *ScienceAsia* **49**, 15–21.
27. Ko HC, Lee JY, Jang MG, Song H, Kim S-J (2018) Seasonal variations in the phenolic compounds and antioxidant activity of *Sasa quelpaertensis*. *Ind Crops Prod* **122**, 506–512.
28. Benzie IF, Strain JJ (1999) Ferric reducing/antioxidant power assay: direct measure of total antioxidant activity of biological fluids and modified version for simultaneous measurement of total antioxidant power and ascorbic acid concentration. *Meth Enzymol* **299**, 15–27.
29. Kumar RA, Sridevi K, Kumar NV, Nanduri S, Rajagopal S (2004) Anticancer and immunostimulatory compounds from *Andrographis paniculata*. *J Ethnopharmacol* **92**, 291–295.
30. Rajagopal S, Kumar RA, Deevi DS, Satyanarayana C, Rajagopalan R (2003) Andrographolide, a potential cancer therapeutic agent isolated from *Andrographis paniculata*. *J Exp Ther Oncol* **3**, 147–158.
31. Li L, Yue GG-L, Lee JK-M, Wong EC-W, Fung K-P, Yu J, Lau CB-S, Chiu PW-Y (2017) The adjuvant value of *Andrographis paniculata* in metastatic esophageal cancer treatment – from preclinical perspectives. *Sci Rep* **7**, 854.
32. Naomi R, Bahari H, Ong ZY, Keong YY, Embong H, Rajandram R, Teoh SH, Othman F, et al (2022) Mechanisms of natural extracts of *Andrographis paniculata* that target lipid-dependent cancer pathways: A view from the signaling pathway. *Int J Mol Sci* **23**, 5972.
33. Vijayarathna S, Sasidharan S (2012) Cytotoxicity of methanol extracts of *Elaeis guineensis* on MCF-7 and Vero cell lines. *Asian Pac J Ttrop Biomed* **2**, 826–829.
34. Indrayanto G, Putra G, Suhud F (2021) Validation of *in-vitro* bioassay methods: Application in herbal drug research. In: Al-Majed AA (ed) *Profiles of Drug Substances, Excipients and Related Methodology*, vol 46, Academic Press, pp 273–307.
35. Elmore S (2007) Apoptosis: a review of programmed cell death. *Toxicol Pathol* **35**, 495–516.
36. Malik Z, Parveen R, Parveen B, Zahiruddin S, Khan M, Khan A, Massey S, Ahmad S, et al (2021) Anticancer potential of andrographolide from *Andrographis paniculata* (Burm.f.) Nees and its mechanisms of action. *J Ethnopharmacol* **272**, 113936.
37. Lee Y-C, Lin H-H, Hsu C-H, Wang C-J, Chiang T-A, Chen J-H (2010) Inhibitory effects of andrographolide on migration and invasion in human non-small cell lung cancer A549 cells via down-regulation of PI3K/Akt signaling pathway. *Eur J Pharmacol* **632**, 23–32.
38. Chi HT, Ly BT, Kano Y, Tojo A, Watanabe T, Sato Y (2012) ETV6-NTRK3 as a therapeutic target of small molecule inhibitor PKC412. *Biochem Biophys Res Commun* **429**, 87–92.